Available online at www.sciencedirect.com
SCIENCE DIRECT®
European Journal of Mechanics B/Fluids 24 (2005) 703–716

The method of fundamental solutions for Stokes flow in a rectangular cavity with cylinders

D.L. Young [a,*], C.W. Chen [a], C.M. Fan [a], K. Murugesan [a], C.C. Tsai [b]

[a] *Department of Civil Engineering & Hydrotech Research Institute, National Taiwan University, Taipei, Taiwan*
[b] *Department of Information Technology, Toko University, Chia-Yi County, Taiwan*

Received 26 August 2004; received in revised form 6 February 2005; accepted 17 March 2005

Available online 5 May 2005

Abstract

Numerical solutions based on the method of fundamental solutions are discussed for Stokes flow inside a rectangular cavity in the presence of circular cylinders. The Stokeslets are used as the fundamental solutions to obtain the solution for the flow field by a linear combination of fundamental solutions. Flow results on the cellular structure of flow field resulting from the dynamics of cylinders and the horizontal walls of the cavity are reported for (i) one rotating cylinder in a rectangular cavity with two parallel horizontal sides moving in the same directions as well as in the opposite directions, (ii) two rotating cylinders kept apart in a rectangular cavity with two parallel horizontal sides moving in the same directions as well as in the opposite directions. The effect of aspect ratio of the rectangular cavity, direction of movement of the two parallel horizontal sides of the cavity and the diameter of the rotating cylinder on the flow structure are studied. The flow results obtained for the single cylinder case are in accordance with the results available in the literature. From the computational point of view, the present numerical procedure based on the method of fundamental solutions is efficient and simple to implement as compared to the mesh-dependent schemes, which needs complex mesh generation procedure for the multiply connected geometrical domains considered in this article.

Keywords: Method of fundamental solutions; Stokeslet; Rectangular cavity; Rotating cylinders

1. Introduction

Theoretical studies of Stokes flow in a rectangular cavity with rotating cylinders provide useful information on distributive mixing which has many industrial applications. Though the flow is dominated only by shear force, the presence of obstacles and the rotation of cylinders produce eddy zones and dead zones which affect the mixing process. For simple flow configurations involving only a moving wall with a stationary cylinder the Stokes equations could be solved directly by analytical method [1]. Sometimes, experimental methods have also been used to understand the complex flow structures created by chaotic mixing produced by discontinuous and sinusoidal flow [2] and shear flow past a circular cylinder with arbitrary rotational speeds [3]. Analytical solutions of Stokes equations for flow domains such as a rectangular cavity with rotating cylinders involve complex solution procedure [4]. Hence Hellou and Coutanceau [4] supported their analytical and numerical predictions with experimental

* Corresponding author. Fax: +886 2 23626114.
E-mail address: dlyoung@ntu.edu.tw (D.L. Young).

0997-7546/$ – see front matter
doi:10.1016/j.euromechflu.2005.03.003

results. In a recent work, Galaktionov et al. [5] solved the bi-harmonic form of the Stokes equations using the method of superposition to study the distributive mixing produced by a circular cylinder placed at the centre of a rectangular cavity. Though the works of Hellou and Coutanceau [4] and Galaktionov et al. [5] demonstrated that analytical and numerical solutions could be achieved for multiply connected flow domains, their methods are not simple from computational point of view.

The present article describes a numerical procedure based on the free-space Green's function, called the method of fundamental solutions (MFS) to solve the Stokes equations in multiply connected flow domains. For flow domains consisting of a rotating cylinder in a rectangular cavity, the application of the domain numerical methods such as the finite volume method (FVM), the finite difference method (FDM) and the finite element method (FEM) will be tedious due to the problem of mesh generation. Meshless numerical schemes such as the MFS will be a promising numerical tool to deal with multiply connected flow domains. The MFS [6–12] has been well established as a potential numerical scheme to solve problems involving singularities in flow problems. Especially, Alves and Silvestre [12] derived density results of the MFS based on the Stokeslet, which provided the mathematical fundamentals of the present works. The MFS does not require the discretization of the interior computational domain like the boundary element method (BEM) but at the same time overcomes the problem of singularity. Since the MFS is free from mesh generation procedure, it is highly suitable to solve flow problems involving multiply connected domains such as found in a mixing problem.

In the present work the MFS is employed to solve Stokes equations using the Stokeslets as the source points since the Stokeslets are the fundamental solutions of Stokes equations. The MFS utilizes the collocation procedure to determine the flow field variables at a selected number of field points using the known boundary conditions. Hence by properly selecting the locations of the source points, flow fields in a computational domain involving multiply connected geometries also can be predicted without the problem of singularity and mesh generation. The present numerical scheme is applied to study Stokes flow in a rectangular cavity with (i) one rotating cylinder and (ii) two rotating cylinders kept apart on the horizontal centerline of the cavity. The details about the governing equations used, the MFS procedure and comparison of results with other numerical methods are discussed in the following sections.

2. Governing equations

The momentum conservation of a fluid medium for creeping flow, where the inertial forces are negligible compared to other forces, can be represented by the 2D Stokes equations as follows:

Continuity

$$\frac{\partial u}{\partial x} + \frac{\partial v}{\partial y} = 0. \tag{1}$$

Momentum

$$0 = -\frac{\partial p}{\partial x} + \mu \nabla^2 u + f_x, \tag{2a}$$

$$0 = -\frac{\partial p}{\partial y} + \mu \nabla^2 v + f_y, \tag{2b}$$

where p is the pressure, u, v are the velocity components in the x and y directions respectively, μ is the dynamic viscosity of the fluid, and f_x, f_y are the external forces in the x and y directions respectively.

The satisfaction of continuity equation guarantees the existence of the stream function for 2D flow field. Hence the relation between the velocities and stream function can be expressed as

$$u = \frac{\partial \psi}{\partial y}, \tag{3}$$

$$v = -\frac{\partial \psi}{\partial x}, \tag{4}$$

where ψ is the stream function.

2.1. Stokeslet

The free-space Green's function is the potential generated by a unit amplitude point source located at a given point in a flow domain. The Stokeslet is the fundamental solution for the Stokes equations and it represents the velocity field due to a

concentrated point force acting in a fluid continuum. Similarly the velocity field that satisfies Stokes equations by the application of a torque at a point is called a rotlet. Hence, if the momentum equation of the Stokes flow can be modified using either a point force or a torque as a singularly forced Stokes equations, then the Green's function can be used to obtain the flow solutions. However, the flow due to rotlet is more singular and more involved than the Stokeslet [13–15]. Since the singularities in the flow field are overcome by the method of collocation, the Stokeslets are preferred as the source points in the present method using the MFS. By enforcing the Stokeslets as the source points, the momentum equation for Stokes flow given by Eq. (2) can be rewritten as follows:

$$-\frac{\partial p^*}{\partial x} + \mu\nabla^2 u^* = -b^x \delta(x - x_0)(y - y_0), \tag{5a}$$

$$-\frac{\partial p^*}{\partial y} + \mu\nabla^2 v^* = -b^y \delta(x - x_0)(y - y_0), \tag{5b}$$

where (b^x, b^y) is the magnitude of the applied force, $\delta(x - x_0)(y - y_0)$ is the well-known Dirac delta function, (x, y) and (x_0, y_0) are the spatial coordinates of the positions of the field point and the source point respectively, and the flow variables with '*' are the variables of the Stokeslet.

For the case of a two-dimensional flow field, the Stokeslet can be represented as the following [12,15,16]:

$$u^* = \frac{1}{8\pi\mu}\left[b^x\left(-2\ln(r) + \frac{2(\hat{x})^2}{r^2} - 3\right) + b^y\left(\frac{2(\hat{x})(\hat{y})}{r^2}\right)\right], \tag{6a}$$

$$v^* = \frac{1}{8\pi\mu}\left[b^x\left(\frac{2(\hat{x})(\hat{y})}{r^2}\right) + b^y\left(-2\ln(r) + \frac{2(\hat{y})^2}{r^2} - 3\right)\right], \tag{6b}$$

$$\psi^* = \frac{1}{8\pi\mu}\left[b^x\left(-2(\hat{y})\ln(r) - (\hat{y})\right) + b^y\left(2(\hat{x})\ln(r) + (\hat{x})\right)\right], \tag{6c}$$

where $r = |\vec{x} - \vec{x}_0|$ is the distance between the source point and the field point and $\hat{x} = x - x_0$ and $\hat{y} = y - y_0$ are the x-coordinate and y-coordinate differences between these two points. It is to be noted that all the above discussions were made without being specific about the boundary conditions. For a well posed boundary value problem the values of all the field variables on the boundary are known and the solution can be obtained using the MFS and the Stokeslet by the method of collocation as discussed in the following section.

3. Application of the method of fundamental solutions (MFS)

The Stokes equations (1) and (2) are linear and hence the method of superposition can be adopted to obtain the numerical solutions. For the linear governing equations, the method of fundamental solutions state that the velocity field can be represented by a linear combination of fundamental solutions of the governing equations. When the Stokeslet is used as the singularity, the numerical procedure becomes much simpler to solve the Stokes equations because Stokeslet itself is the fundamental solution for the Stokes equations. Also in order to avoid the problem of singularity, the source points are placed at some distance outside the computational domain on an artificial boundary with different strengths. By making use of the Stokeslet expressed by Eqs. (6a–c), the velocity fields can be expressed by a linear combination of the fundamental solutions as

$$u(\vec{x}_i) = \frac{1}{8\pi\mu}\left[\sum_{j=1}^{N}\alpha_j^x\left(-2\ln(r_{ij}) + \frac{2(x_i - x_j)^2}{r_{ij}^2} - 3\right) + \sum_{j=1}^{N}\alpha_j^y\left(\frac{2(x_i - x_j)(y_i - y_j)}{r_{ij}^2}\right)\right], \tag{7a}$$

$$v(\vec{x}_i) = \frac{1}{8\pi\mu}\left[\sum_{j=1}^{N}\alpha_j^x\left(\frac{2(x_i - x_j)(y_i - y_j)}{r_{ij}^2}\right) + \sum_{j=1}^{N}\alpha_j^y\left(-2\ln(r_{ij}) + \frac{2(y_i - y_j)^2}{r_{ij}^2} - 3\right)\right], \tag{7b}$$

where N is the number of source points, α_j^x and α_j^y are the strength coefficients to be determined in the x and y directions respectively. The boundary conditions for the velocity components will be collocated on a selected number of field points on the boundary to determine the unknown coefficients (α_j^x, α_j^y). After obtaining the values of these coefficients, the velocity field of the domain can be obtained using Eqs. (7a) and (7b), whereas the stream function can be determined using the following equation:

$$\psi(\vec{x}_i) = \frac{1}{8\pi\mu}\left[\sum_{j=1}^{N}\alpha_j^x\left(-2(y_i - y_j)\ln(r_{ij}) - (y_i - y_j)\right) + \sum_{j=1}^{N}\alpha_j^y\left(2(x_i - x_j)\ln(r_{ij}) + (x_i - x_j)\right)\right]. \tag{7c}$$

Finally the numerical solution procedure reduces to the determination of the coefficients α_j^x and α_j^y. It is to be noted that the coefficients α_j^x and α_j^y in Eqs. (7a–c) are the same for both the velocities and the stream function. If the given problem possesses a unique solution, then the values of these coefficients will also be unique for a given set of boundary conditions. This is because the MFS is derived using the free-space Green's function, considered as the potential generated by a unit amplitude source point located on an artificial boundary, which is forced to satisfy the appropriate boundary conditions. Hence the coefficients α_j^x and α_j^y represent the same flow field and are common to all the flow variables for a given set of boundary conditions. Using the method of collocation, Eqs. 7(a) and 7(b) can be written as matrix equations for a given number of N field points on the boundary and can be represented as

$$[A_{ij}] \begin{Bmatrix} \alpha_j^x \\ \alpha_j^y \end{Bmatrix} = \begin{Bmatrix} u_{i,\Gamma} \\ v_{i,\Gamma} \end{Bmatrix}. \tag{8}$$

With the imposition of known velocity values on the boundary at the right-hand side of the above equation, the values of the coefficients α_j^x and α_j^y can be obtained from Eq. (8) after evaluating the coefficient matrix $[A_{ij}]$. Once the coefficients α_j^x and α_j^y are determined the boundary values of the flow field variables can be verified by treating them as internal domain values just coinciding with the boundary. Then the flow field variables on the other field points in the interior domain everywhere can be computed directly using Eqs. 7(a–c).

4. Numerical results

In order to validate the proposed numerical scheme based on the MFS and the Stokeslet, some validation problems, for which results are available in the literature, are simulated. Flow results are compared qualitatively with other works in the form of streamlines patterns. In addition to this velocity values, other flow parameters computed at some selected flow boundaries are quantitatively compared with results available in the literature. The numerical capability of the proposed scheme is also demonstrated by extending the simulation to study some problems that resemble distributive mixing.

Table 1
Comparison of velocity on the boundaries of cylinders and channel

Velocity values on the boundary ($N = 100$), $R_0 = 0.3$									
Channel wall					Cylinder boundary				
x	y	MFS	Analytical	Error (%)	x	y	MFS	Analytical	Error (%)
−5.00	−4.75	0.000000001	0.000000000	1.00E−07	1.50	0.06	5E−09	0.000000000	5.00E−07
−5.00	−2.25	0.000000002	0.000000000	2.00E−07	1.36	0.64	1E−09	0.000000000	1.00E−07
−5.00	0.25	0.000000002	0.000000000	2.00E−07	1.01	1.11	1E−09	0.000000000	1.00E−07
−5.00	2.75	0.000000001	0.000000000	1.00E−07	−0.09	1.50	4E−09	0.000000000	4.00E−07
−5.00	4.75	0.000000002	0.000000000	2.00E−07	−1.13	0.98	3E−09	0.000000000	3.00E−07
−4.75	5.00	10.000000000	10.000000000	0.00E+00	−1.50	−0.12	3E−09	0.000000000	3.00E−07
−2.25	5.00	9.999999999	10.000000000	1.00E−07	−0.96	−1.15	1E−08	0.000000000	1.10E−06
0.25	5.00	10.000000006	10.000000000	6.00E−07	0.15	−1.49	1E−09	0.000000000	1.00E−07
2.75	5.00	10.000000001	10.000000000	1.00E−07	1.17	−0.94	9E−09	0.000000000	9.00E−07
4.75	5.00	9.999999999	10.000000000	1.00E−07	1.50	0.06	5E−09	0.000000000	5.00E−07
Velocity values on the boundary ($N = 100$), $R_0 = 0.1$									
Channel wall					Cylinder boundary				
x	y	MFS	Analytical	Error (%)	x	y	MFS	Analytical	Error (%)
−5.00	−4.75	0.000000009	0.000000000	9.00E−07	0.50	0.02	0.000000005	0.000000000	5.00E−07
−5.00	−2.25	0.000000012	0.000000000	1.20E−06	0.45	0.21	0.000000005	0.000000000	5.00E−07
−5.00	0.25	0.000000018	0.000000000	1.80E−06	0.34	0.37	0.000000007	0.000000000	7.00E−07
−5.00	2.75	0.000000015	0.000000000	1.50E−06	−0.03	0.50	0.000000012	0.000000000	1.20E−06
−5.00	4.75	0.000000019	0.000000000	1.90E−06	−0.38	0.33	0.000000006	0.000000000	6.00E−07
−4.75	5.00	9.999999981	10.000000000	1.90E−06	−0.50	−0.04	0.000000008	0.000000000	8.00E−07
−2.25	5.00	9.999999966	10.000000000	3.40E−06	−0.32	−0.38	0.000000008	0.000000000	8.00E−07
0.25	5.00	9.999999981	10.000000000	1.90E−06	0.05	−0.50	0.000000010	0.000000000	1.00E−06
2.75	5.00	9.999999984	10.000000000	1.60E−06	0.39	−0.31	0.000000009	0.000000000	9.00E−07
4.75	5.00	9.999999991	10.000000000	9.00E−07	0.50	0.02	0.000000005	0.000000000	5.00E−07

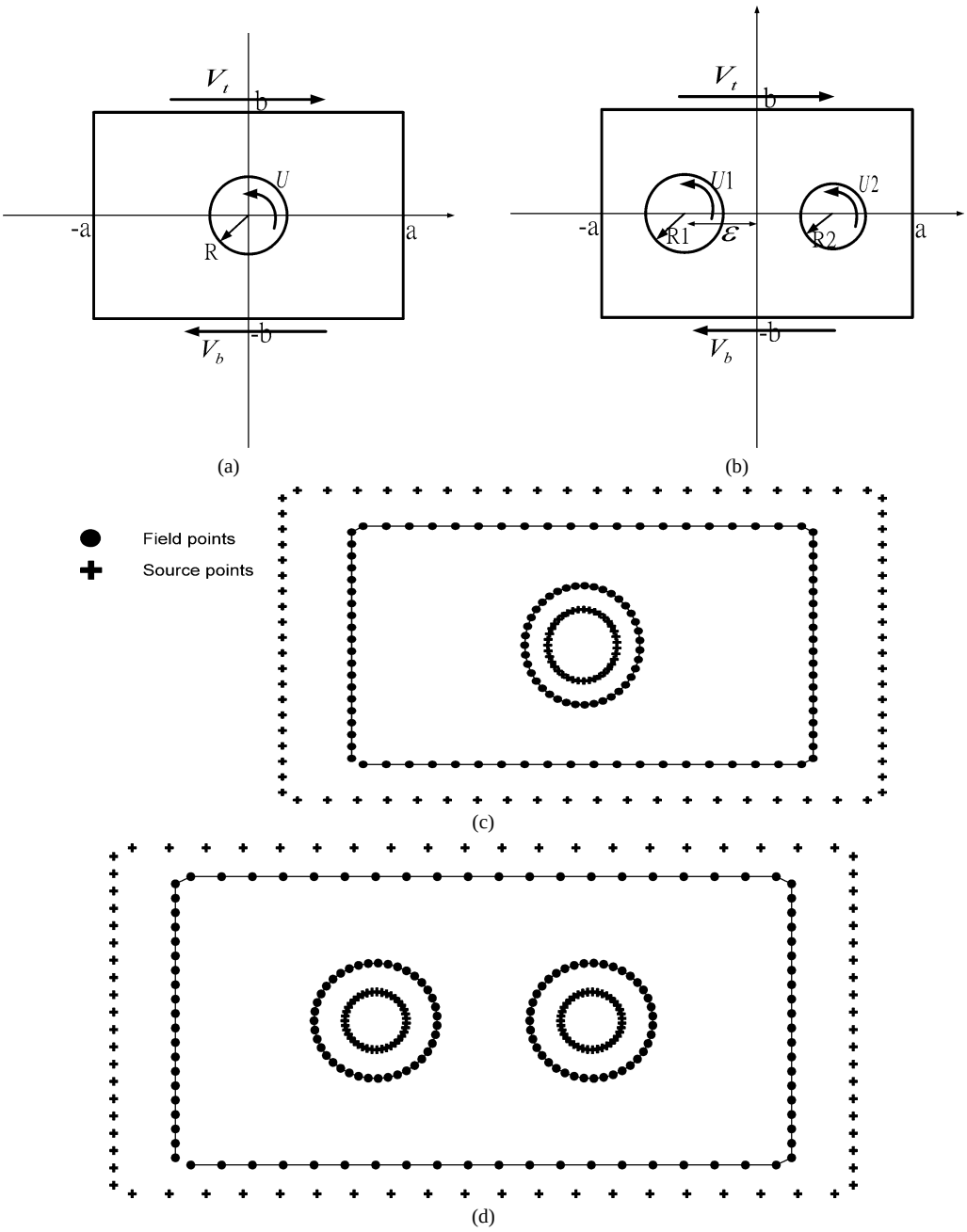

Fig. 1. Schematic diagram for Stokes flow (a) two moving walls and a rotating cylinder, (b) two moving walls and two rotating cylinders, (c) field points and source points distribution for case (a), (d) field points and source points distribution for case (b).

4.1. Validation results

For validation purpose, the Stokes flow problems studied by Hellou and Coutanceau [4] and Galaktionov et al. [5] are considered. The problem consists of studying the eddy formation in a rectangular cavity with a cylinder placed at the centre of the cavity. The ratio of the width to height of the cavity is defined as the aspect ratio, H, of the cavity. The radius of the cylinder is defined as R and R_0 is the ratio of the width to the radius. It is assumed that the top and the bottom walls of the cavity will be moving with velocities V_t and V_b respectively, whereas the velocity of the cylinder is assumed to be equal to U for the case of a single cylinder and $U1$ and $U2$ for the case of two cylinders. These velocities are represented in terms of a reference

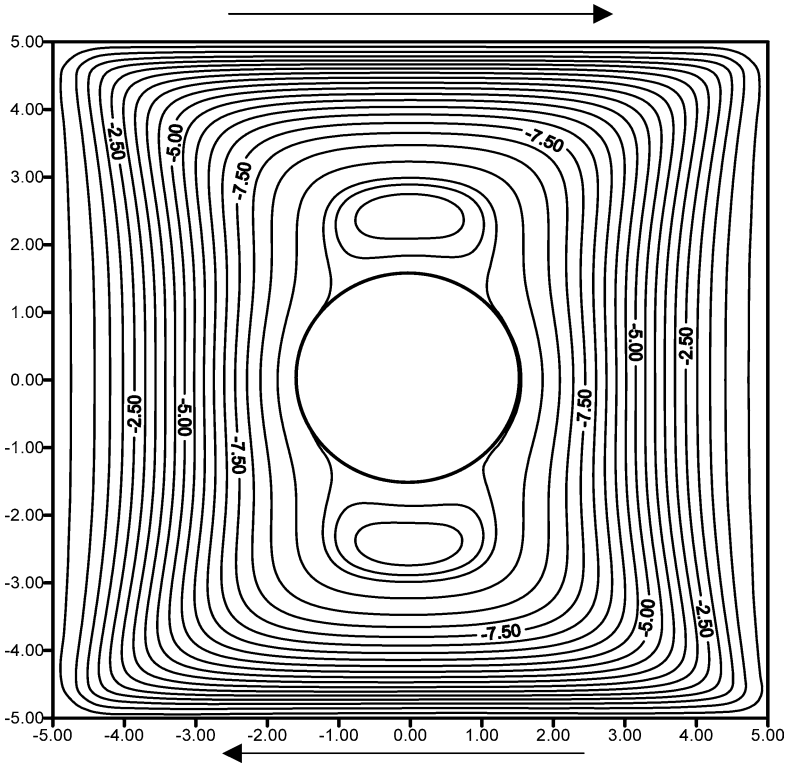

(a)

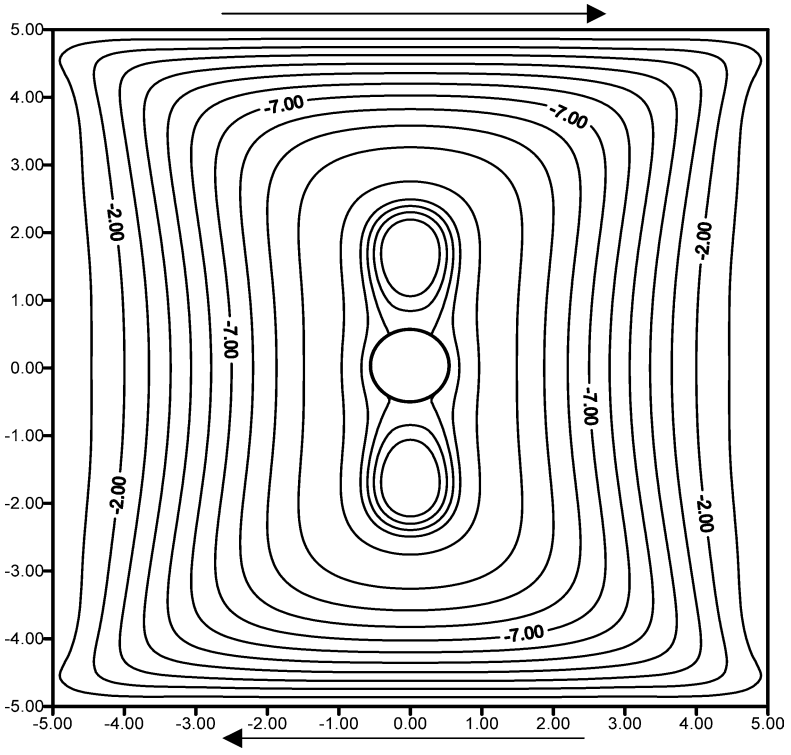

(b)

Fig. 2. Streamline patterns for cavity flow with $V_t = V = -V_b$, $U = 0$ ($V = 10$, $H = 1$, $N = 120$) (a) $R_0 = 0.3$, (b) $R_0 = 0.1$.

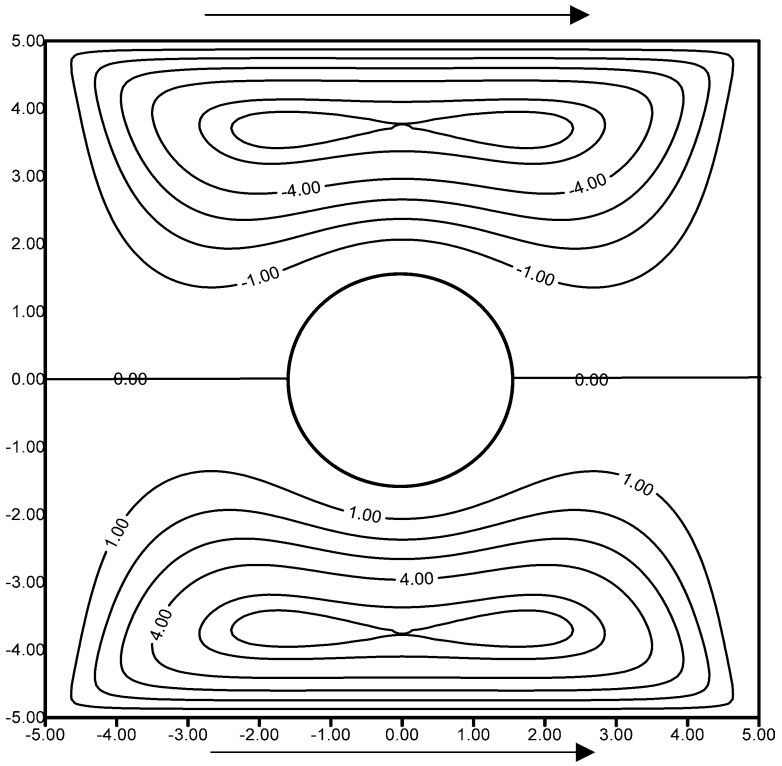

(a)

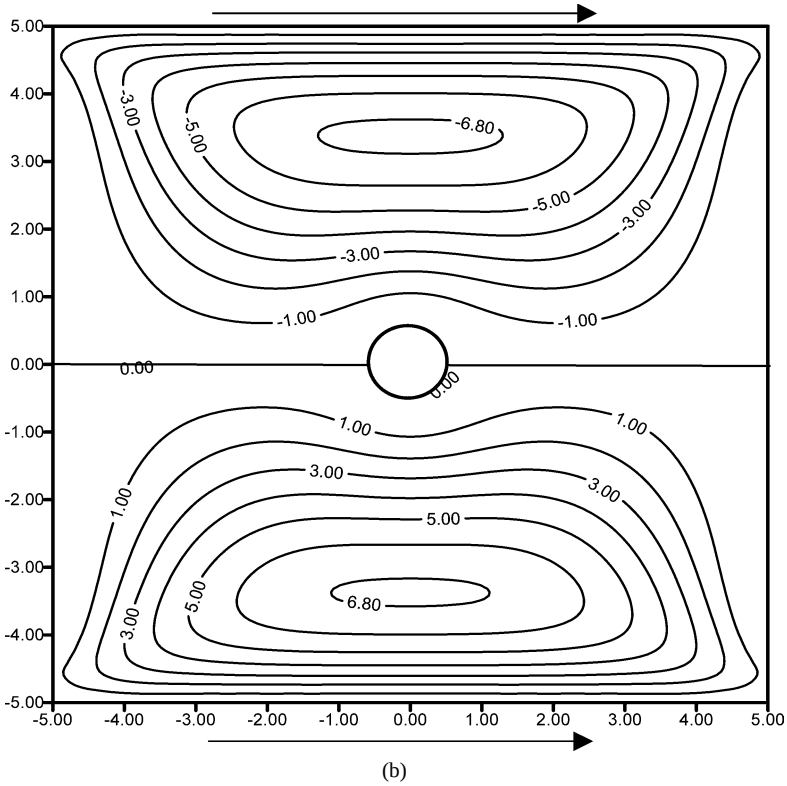

(b)

Fig. 3. Streamline patterns for cavity with $V_t = V_b = V$, $U = 0$ ($V = 10$, $H = 1$, $N = 120$) (a) $R_0 = 0.3$, (b) $R_0 = 0.1$.

Table 2
Comparison of results with Ref. [5]

Coordinates of point (x, y) inside the cavity						
Result of Ref. [5]	$(0.6a, 0)$		$(0.6a, 0.8b)$		$(0, 0.8b)$	
	U_x	U_y	U_x	U_y	U_x	U_y
Ref. resultl	0.00000	−0.40180	0.47690	−0.08040	0.73940	0.00000
Ref. result2	0.00000	−0.40180	0.47690	−0.08040	0.73940	0.00000
Ref. results	0.00000	−0.40180	0.47700	−0.08040	0.73930	0.00000
MFS	0.00007	−0.40120	0.47810	−0.08010	0.74000	0.00005
Error (%)	–	1.49E−01	2.52E−01	3.73E−01	8.11E−02	–

Table 3
Comparison of velocity on channel wall with Ref. [4]

Mean value of the velocity on the channel walls		
Aspect ratio	Velocity	
	Ref. [4]	MFS ($N = 120$)
1.0	5.40E−07	2.59E−07
1.5	1.60E−07	3.06E−08
2.0	1.70E−07	1.19E−07
2.5	5.40E−07	7.69E−07
3.0	2.40E−06	2.44E−06
3.5	9.60E−06	7.36E−07

Table 4
Comparison of corner cell position with Ref. [4]

Evolution of the lengths of the sides of the first corner cell				
Aspect ratio	lateral direction		transverse direction	
	Ref. [4]	MFS	Ref. [4]	MFS
1.3	0.40	0.40	0.42	0.42
1.4	0.49	0.49	0.59	0.60
1.5	0.60	0.61	1.00	1.00

Table 5
Error values of the MFS predictions

Velocity values on the boundary ($N = 120$)									
Channel wall					Cylinder boundary				
x	y	MFS	Analytical	Error (%)	x	y	MFS	Analytical	Error (%)
−10.00	−4.50	0.000015925	0.000000000	1.59E−03	−3.468	1.403	7.500002129	7.500000000	2.13E−04
−10.00	0.50	0.000006829	0.000000000	6.83E−04	−5.199	0.901	7.499995283	7.500000000	4.72E−04
−9.00	5.00	9.999996778	10.000000000	3.22E−04	−5.199	−0.901	7.499998390	7.500000000	1.61E−04
1.00	5.00	10.000001171	10.000000000	1.17E−04	−3.468	−1.403	7.499998973	7.500000000	1.03E−04
10.00	4.50	0.000005843	0.000000000	5.84E−04	−2.505	0.121	7.500007883	7.500000000	7.88E−04
10.00	−0.50	0.000005921	0.000000000	5.92E−04	4.532	1.403	7.500002815	7.500000000	2.82E−04
9.00	−5.00	10.000000216	10.000000000	2.16E−05	2.801	0.901	7.499997645	7.500000000	2.36E−04
−1.00	−5.00	10.000003890	10.000000000	3.89E−04	2.801	−0.901	7.499996901	7.500000000	3.10E−04
−5.00	−5.00	9.999998285	10.000000000	1.71E−04	4.532	−1.403	7.500001850	7.500000000	1.85E−04
−9.00	−5.00	9.999996207	10.000000000	3.79E−04	5.495	0.121	7.500004307	7.500000000	4.31E−04

velocity V, which is assumed in the order of 10 in the present work. The number of field points (N) is assumed to be equal to the number of source points and this value is provided in all the figures. The following sections discuss on the MFS results obtained on the flow structures due to the effect of (i) velocity and direction of the moving top and bottom walls of the cavity, (ii) radius of the cylinder, (iii) velocity and direction of the cylinder [5] and (iv) aspect ratio of the cavity [4]. Fig. 1(a) shows the schematic diagram of the Stokes flow for the validation problem. The location of the field points and the source points that are defined by the Stokeslet in the MFS procedure are shown in Fig. 1(c).

4.2. Case 1: Square cavity with a single fixed cylinder

The effect of cylinder radius on the flow structures is predicted by the MFS for the cavity with top and bottom sides moving in the opposite directions and are shown as streamline patterns in Fig. 2(a) and 2(b) for cylinder radius $R_0 = 0.3$ and $R_0 = 0.1$ respectively. The MFS correctly simulated the formation of two eddy zones attached to the cylinder. Table 1 shows the comparisons between the velocity values obtained by the MFS and the analytical solutions at some selected number of field points on the cylinders as well as on the channel wall. The MFS predicted the velocities very closer to the analytical solutions.

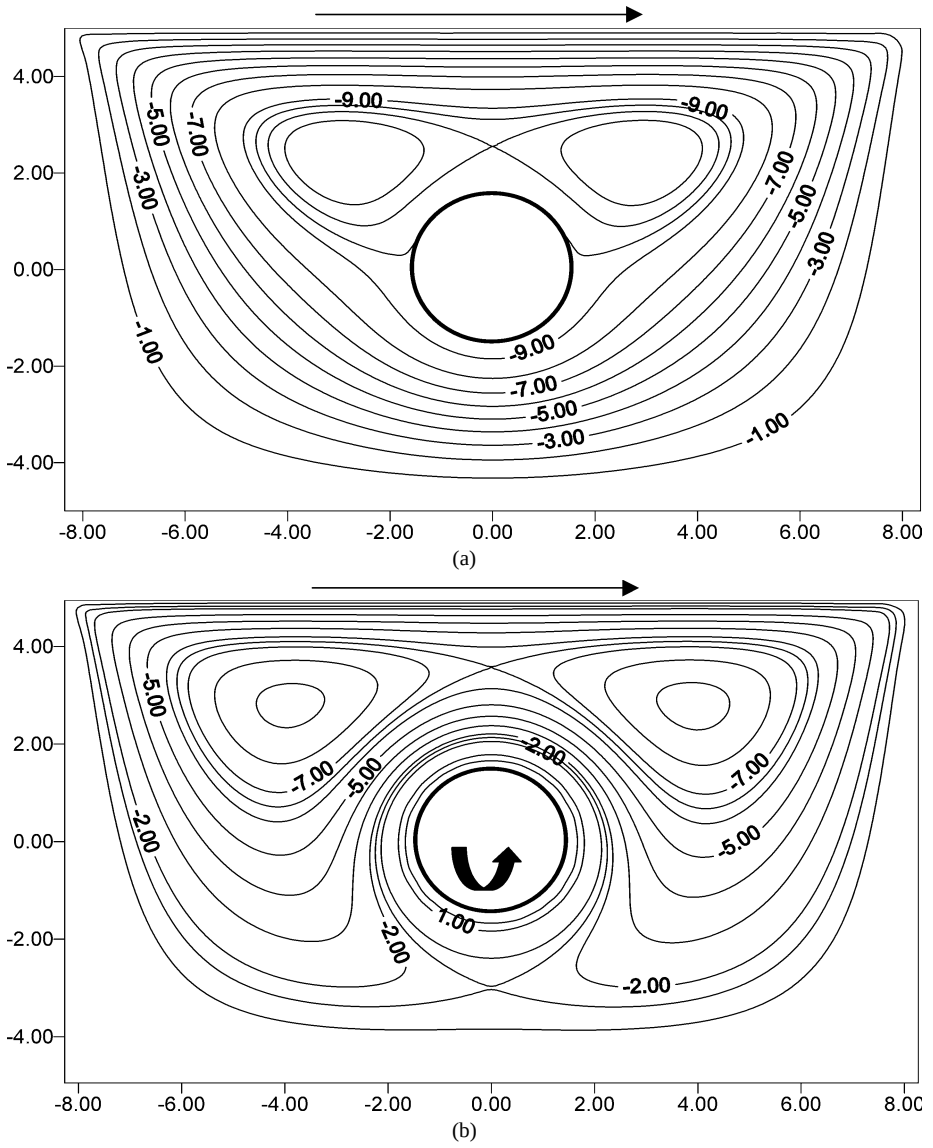

Fig. 4. Streamline patterns for cavity with $V_b = 0$, $V_t = V$ ($V = 10$, $H = 1.67$, $R_0 = 0.3$, $N = 160$) (a) $U = 0$ (b) $U = 0.9V$.

When the top and the bottom horizontal walls of the cavity are moving in the same directions, two symmetric flow sub-domains, on the upper and the lower parts of the cylinder are produced by the streamline patterns as observed in Fig. 3(a). Each sub-domain is formed by two eddies enclosed by a separatrix, which passes through a saddle type stagnation point. With decrease in cylinder radius, the two eddies formed on either sides of the cylinder merge as observed in Fig. 3(b).

4.3. Case 2: Rectangular cavity with a single cylinder

Fig. 4(a) shows the streamline patterns predicted by the MFS when the cylinder is fixed. Due to the movement of the top wall of the cavity, a flow zone with two eddies attached to the cylinder are observed on the side of the moving wall as depicted in the above figure. When the cylinder is made to rotate in a direction opposite to that of the moving top wall of the cavity, the eddy zone with the pair of eddies is separated from the cylinder as depicted by the streamline patterns in Fig. 4(b). As seen from Fig. 4(b) a stagnation point arises at the bottom half of the cavity resulting in a “dog snout” streamline pattern. The streamline patterns predicted by the MFS for Case (1) and Case (2) produced the expected flow structures. The velocity values compared

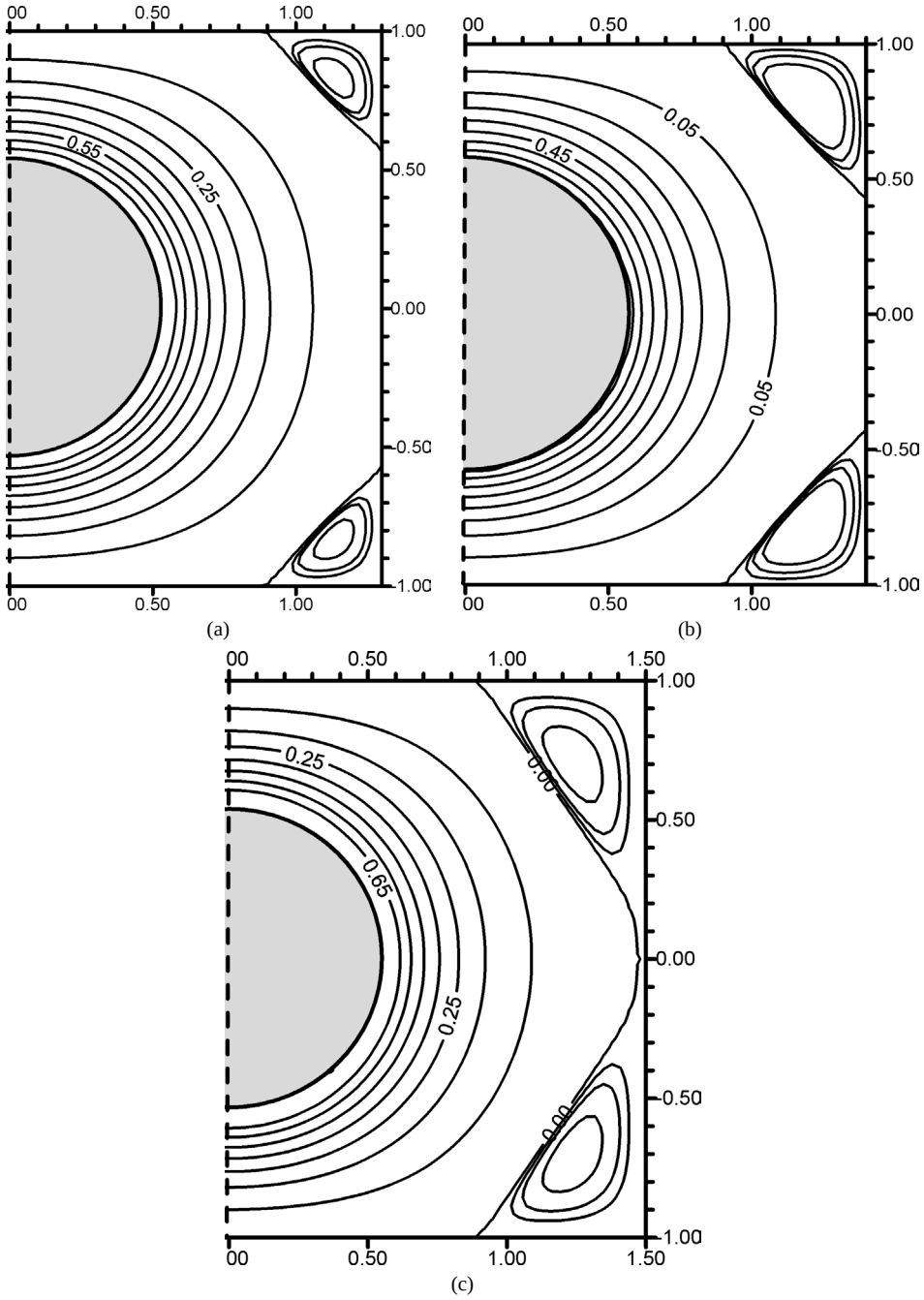

Fig. 5. Flow structures during the evolution of the first corner cells for aspect ratios (a) 1.3, (b) 1.4 and (c) 1.5 ($N = 180$).

in Table 2 are also in good agreement with those of Galaktionov et al. [5]. The streamline patterns predicted by the MFS for the above two validation cases are in qualitative agreement with the results of Galaktionov et al. [5].

Further the mean values of the velocity on the channel walls predicted by the MFS for different aspect ratios show good comparisons with the results of Hellou and Coutanceau [4] as shown in Table 3. The MFS results for the corner cell positions computed as a function of aspect ratio also show close agreement with the above reference as shown in Table 4. Moreover, the numerical accuracy of the MFS scheme for the above tabular values can be verified from the streamline patterns shown in Figs. 5(a)–(c) for aspect ratios (width/height) 1.3, 1.4, and 1.5 respectively. The flow structures starting from the evolution of

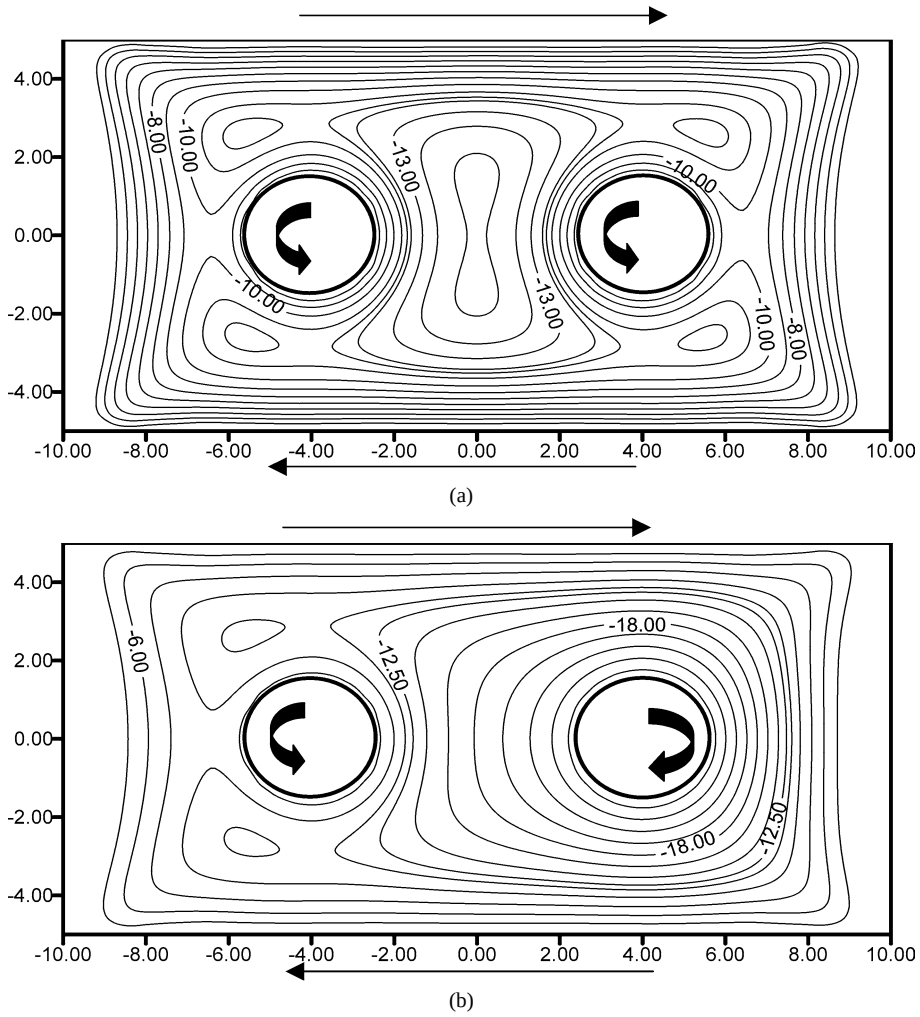

Fig. 6. (a) Streamline patterns for cavity with $V_t = V = -V_b$, $U1 = U2 = 0.075V$ ($V = 10$, $H = 1.67$, $R_0 = 0.3$, $N = 200$), (b) Streamline patterns for cavity with two rotating cylinders with $V_t = V = -V_b$, $U1 = -U2 = 0.075V$ ($V = 10$, $H = 1.67$, $R_0 = 0.3$, $N = 200$).

the Moffat corner cells and the growth of the corner cells with increase in the aspect ratio are correctly predicted and are in qualitative comparison with Ref. [4].

4.4. Test problem 1: Rectangular cavity with two cylinders

After validating the numerical scheme the method is extended to study the flow structures generated in a rectangular cavity with two moving cylinders of equal radius $R_0 = 0.3$. Fig. 1(b) describes the schematic diagram of the Stokes flow for this test problem. The location of the field points and the source points that are defined by the Stokeslet in the MFS procedure are shown in Fig. 1(d). The top and bottom walls of the cavity are assumed to move with the same velocity but in the opposite directions. The effect of the direction of the rotating cylinders on the flow structure is studied. The cylinders are placed in the horizontal central line along the vertical mid line of the cavity, each placed from the end wall at a distance of $3/4$th the distance between the cylinders in the horizontal direction. Fig. 6(a) shows the streamline patterns inside the cavity when the two cylinders rotate in the same directions. The figure indicates the formation of an eddy zone at the middle of the space between the two rotating cylinders and the eddy zone is separated from the rest of the flow regime. Due to the movement of the top and the bottom walls and the two rotating cylinders, the eddy zone looks squeezed along the vertical direction. The comparisons of velocity values predicted by the MFS and the analytical solutions at a selected number of boundary points on the channel are shown in Table 5. The tabular values indicate that the velocity values predicted by the MFS are in close agreement with the analytical solutions. Similarly the velocity values on the cylinder boundary are also predicted very closer to the values of the analytical solutions.

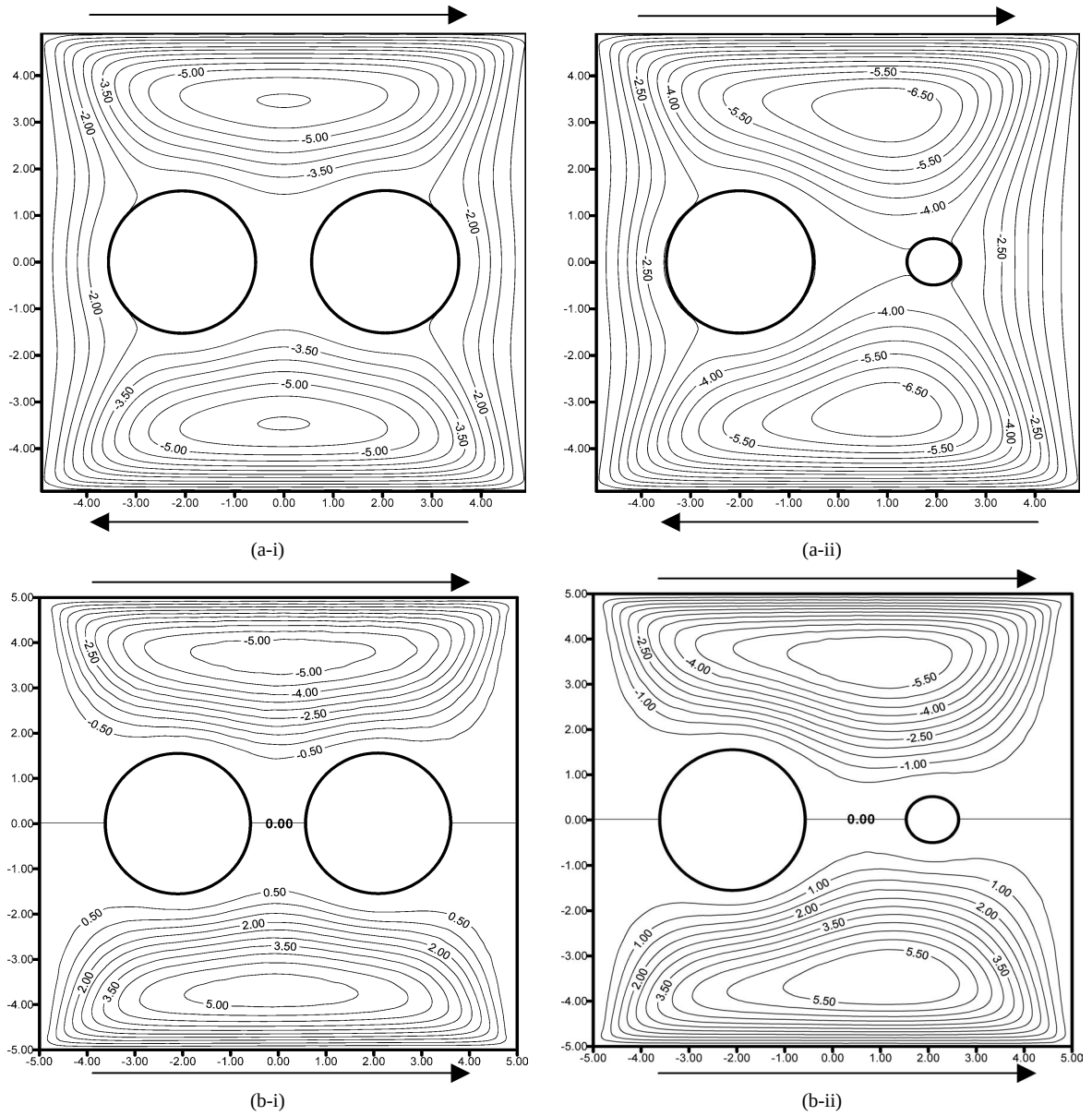

Fig. 7. Streamline patterns for (a) $V_t = V = -V_b$, $U1 = U2 = 0$ (i) $R_{01} = R_{02} = 0.3$, (ii) $R_{01} = 0.3$, $R_{02} = 0.1$ ($V = 10$, $N = 150$) (b) $V_t = V_b = V$, $U1 = U2 = 0$ (i) $R_{01} = R_{02} = 0.3$, (ii) $R_{01} = 0.3$, $R_{02} = 0.1$ ($V = 10$, $N = 150$).

Fig. 6(b) shows the streamline patterns obtained when both the cylinders rotate in the opposite directions. The figure clearly depicts the formation of a weak eddy zone near the left cylinder. The movement of the top wall has a pronounced effect on the velocity distribution near the right cylinder due to the end wall effect produced by the movement of the top wall from left to right. Since the aspect ratio is greater than unity, the end wall effect due to the top wall is not sufficient enough to avoid the eddy formation.

4.5. Test problem 2: Square cavity with two fixed cylinders

A cavity with aspect ratio $H = 1$ is considered with two fixed cylinders kept apart along the horizontal centre line of the cavity as described in the test problem 1. The variations in the flow structures due to the changes in the direction of the movement of horizontal walls of the cavity and the radius of the fixed cylinders are studied. Fig. 7(a-i) shows the streamline patterns for

the cavity with cylinders of equal radius, $R_0 = 0.3$ when the horizontal walls move in the opposite directions. Since the aspect ratio is 1 and the cylinder radii are equal, the end wall effect of the moving walls produce similar streamline patterns near both the cylinders as seen from the above figure. As the cylinders are fixed and only the horizontal walls are moving, two eddy zones are formed in the upper and lower parts of the cylinders. These flow structures are affected because the two fixed cylinders provide enough non-slip boundary surfaces, thus preventing the penetration of the fluid from the upper region of the cylinders to the lower region. When the diameter of the right cylinder is reduced, the fluid penetration is allowed to take place towards the lower parts of the cylinders as shown by the streamline patterns in Fig. 7(a-ii). The shape of the two eddies formed at the upper and lower parts of the cylinder are stretched towards the right cylinder since its radius is smaller than that of the left cylinder.

The flow simulation is repeated by keeping the top and bottom walls of the cavity moving in the same directions from left to right. Fig. 7(b-i) shows the streamline patterns when the radii of both the cylinders are equal. This flow configuration gives rise to the formation of two eddies, one on each side of the cylinders along the vertical direction. These eddies are completely detached from each other staying closer to the moving walls. This indicates that in such situations, the dead zones formed between these two eddies will retard the mixing process. Comparing Figs. 7(a-i) and 7(b-i) one can easily understand that the mixing process will be enhanced when the horizontal walls of the cavity move in the opposite directions. Fig. 7(b-ii) depicts the streamline patterns when the radius of the right cylinder is reduced. The eddies are stretched towards the right cylinder as expected in this case. Since the horizontal walls are moving in the same directions, the reduction in the diameter of the right cylinder has not produced the expected merging of the two eddies, resulting in poor mixing. The results discussed for the two test problems demonstrate that the numerical scheme based on the MFS is capable of predicting the flow structures generated by two cylinders in accordance to the physics underlying the problem. In these numerical experiments it is found that the present scheme is able to predict flow solutions correctly up to an aspect ratio of 5. Beyond this, the resulting simultaneous equations become highly ill-conditioned and hence some special techniques such as domain decomposition method have to be used to solve the equations.

5. Conclusions

The method of fundamental solutions (MFS) and the Stokeslet are combined to yield a simple numerical scheme for solving two dimensional Stokes flow problems in multiply connected flow domains. Since the MFS is free from mesh discretization at the interior domain and boundary integration, the method is found to be a powerful numerical tool to solve flow problems involving multiple flow domains. The proposed numerical scheme is validated by predicting flow structures produced as a result of relative movement of the top and bottom walls of a cavity with varying aspect ratio and a single cylinder located at the center of the cavity. Apart from the qualitative agreement observed for the streamline patterns with previous works, the numerical predictions of velocities on the boundary also show close agreement with other numerical schemes. The evolution of the Moffat corner cells and the growth of the corner cells with increase in the aspect ratio are also correctly predicted. For problems involving two fixed cylinders, the eddy zones produce better fluid mixing when the horizontal walls of the cavity move in the opposite directions than in the same directions. The results presented in this work demonstrate the capability of the MFS and the Stokeslet to correctly predict the complex flow structures that resemble the distributive mixing phenomena.

Acknowledgements

The National Science Council of Taiwan is gratefully acknowledged for providing the financial support to carry out the present research under the grant no. NSC-93-2611-E-002-001. We also like to thank all the three reviewers for suggesting very valuable and constructive comments to improve our paper, it is highly appreciated.

References

[1] D.J. Jeffrey, J.D. Sherwood, Streamline patterns and eddies in low-Reynolds-number flow, J. Fluid Mech. 96 (1980) 315–334.
[2] C.W. Leong, J.M. Ottino, Experiments on mixing due to chaotic advection in a cavity, J. Fluid Mech. 209 (1989) 463–499.
[3] C.R. Robertson, A. Acrivos, Low Reynolds number shear flow past a rotating circular cylinder. Part 1. Momentum transfer, J. Fluid Mech. 40 (1970) 685–704.
[4] M. Hellou, M. Coutanceau, Cellular Stokes flow induced by rotation of a cylinder in a closed channel, J. Fluid Mech. 236 (1992) 557–577.
[5] O.S. Galaktionov, V.V. Meleshko, G.W.M. Peters, H.E.H. Meijer, Stokes flow in a rectangular cavity with a cylinder, Fluid Dynamics Res. 24 (1999) 81–102.
[6] C.C. Tsai, D.L. Young, A.H.-D. Cheng, Meshless BEM for three-dimensional Stokes flows, Comput. Modeling Engrg. Sci. 3 (2002) 117–128.

[7] M.A. Golberg, C.S. Chen, H. Bowman, H. Power, Some comments on the use of radial basis functions in the dual reciprocity method, Comput. Mech. 21 (1998) 141–148.
[8] Y.S. Smyrlis, A. Karageorghis, Some aspects of the method of fundamental solutions for certain harmonic problems, J. Sci. Comput. 16 (2001) 341–371.
[9] A. Karageorghis, The method of fundamental solutions for the calculation of the eigenvalues of the Helmholtz equation, Appl. Math. Lett. 14 (2001) 837–842.
[10] A. Poullikkas, A. Karageorghis, G. Grorgiou, Methods of fundamental solutions for harmonic and biharmonic boundary value problems, Comput. Mech. 21 (1998) 416–423.
[11] C.C. Tsai, Meshless numerical methods and their engineering applications, PhD Thesis, Department of Civil Engineering, National Taiwan University, Taipei, Taiwan, 2003.
[12] C.J.S. Alves, A.L. Silvestre, Density results using Stokeslets and a method of fundamental solutions for the Stokes equations, Eng. Anal. Bound. Elem. 28 (2004) 1245–1252.
[13] H. Flores, E. Lobation, S. Mendez-Diez, S. Tlupova, R. Cortez, A study of bacterial flagellar bundling, Bull. Math. Biol, in press.
[14] I.G. Currie, Fundamental Mechanics of Fluids, McGraw-Hill, Boston, 1993.
[15] C. Pozrikidis, Boundary Integral and Singularity Methods for Linearized Viscous Flow, Cambridge University Press, New York, 1992.
[16] O.A. Ladyzhenskaya, The Mathematical Theory of Viscous Incompressible Flow, Gordon and Breach, New York, 1969.